OPEN

Archaeal proteins Nop10 and Gar1 increase the catalytic activity of Cbf5 in pseudouridylating tRNA

Rajashekhar Kamalampeta & Ute Kothe

Department of Chemistry and Biochemistry, University of Lethbridge, Lethbridge, AB, T1K 3M4, Canada.

Cbf5 is a pseudouridine synthase that usually acts in a guide RNA-dependent manner as part of H/ACA small ribonucleoproteins; however archaeal Cbf5 can also act independently of guide RNA in modifying uridine 55 in tRNA. This guide-independent activity of Cbf5 is enhanced by proteins Nop10 and Gar1 which are also found in H/ACA small ribonucleoproteins. Here, we analyzed the specific contribution of Nop10 and Gar1 for Cbf5-catalyzed pseudouridylation of tRNA. Interestingly, both Nop10 and Gar1 not only increase Cbf5's affinity for tRNA, but they also directly enhance Cbf5's catalytic activity by increasing the k_{cat} of the reaction. In contrast to the guide RNA-dependent reaction, Gar1 is not involved in product release after tRNA modification. These results in conjunction with structural information suggest that Nop10 and Gar1 stabilize Cbf5 in its active conformation; we hypothesize that this might also be true for guide-RNA dependent pseudouridine formation by Cbf5.

Pseudouridine synthases are found in all domains of life as they catalyze the formation of the most abundant RNA modification, the site-specific conversion of uridines to pseudouridines. Based on their structure and sequence similarities, pseudouridine synthases are classified into six families named by their bacterial representatives, TruA, TruB, TruD, RsuA and RluA[1] as well as the unrelated pseudouridine synthase Pus10 found in archaea and some eukaryotes[2]. The diversity of pseudouridine synthases allows them to site-specifically target cellular RNAs such as ribosomal RNA, tRNA as well as small nuclear and small nucleolar RNA in eukaryotes. Typically, stand-alone pseudouridine synthases functioning as a single protein recognize one or a small number of related substrate RNA based on structure and/or sequence[1]. In addition, archaea and eukaryotes harbor H/ACA small ribonucleoproteins comprised of the pseudouridine synthase Cbf5 (dyskerin in humans), the accessory proteins Nop10, Gar1 and archaeal L7Ae or eukaryotic Nhp2 as well as an H/ACA guide RNA[3,4]. Here, the different H/ACA guide RNAs are responsible for recruiting the target RNAs through specific base-pairing interactions while Cbf5 remains the catalytic component of the complex[5]. However, the role of the accessory proteins Nop10, Gar1 and L7Ae has not yet been fully established.

Pseudouridines are characterized by a C-C glycosidic bond and an additional imino group in the base which can participate in additional hydrogen bonds. Presumably, these types of additional interactions confer the increased stability to RNA containing pseudouridines[6]. Furthermore, pseudouridines near the active centers of the spliceosome and the ribosome have been implicated in the function of these molecular machines[7,8]. While the exact details of the catalytic mechanism are still under investigation, it is very likely that all pseudouridine synthases employ the same mechanism for pseudouridylation[9] since all pseudouridine synthases share a structurally very similar catalytic domain including a strictly conserved aspartate residue which may form a covalent bond to the ribose[10]. In addition, the active site of pseudouridine synthases is composed of a positively charged residue that interacts with the catalytic aspartate, and an aromatic residue which forms stacking interactions with the uracil ring[1]. In agreement with the suggested common catalytic mechanism, we have recently shown that three families of bacterial pseudouridine synthases are characterized by a uniformly slow catalytic step[11].

Cbf5 is the most complex pseudouridine synthase as it is acting in conjunction with a guide RNA and proteins Nop10, Gar1, and archaeal L7Ae. The structure of the *Pyrococcus furiosus* H/ACA small ribonucleoprotein in presence and absence of substrate RNA provided insight into the molecular architecture of the complex and suggested possible functions of its components[12,13]. As mentioned, Cbf5 is the catalytic unit and interacts extensively with the guide RNA. Nop10 binds to Cbf5 close to the active site and has been proposed to stabilize it, but it also forms some contacts to the guide RNA. Without Nop10, the H/ACA small ribonucleoprotein is inactive in

modifying target RNA[14,15]. Gar1 is the only protein not directly interacting with RNA, instead it can bind to the thumb loop of Cbf5 stabilizing it in an open conformation. Omission of Gar1 limits the guide RNA-dependent pseudouridylation activity of H/ACA small ribonucleoproteins to a single round[12], presumably because product release is impaired when Gar1 is not inducing an open conformation of the thumb loop. Lastly, L7Ae binds to the kink-turn motif in archaeal H/ACA guide RNA thereby helping to position the guide RNA and the substrate RNA within the complex[16]. Interestingly, archaeal Cbf5 is also able to act in a guide RNA-independent manner as it can on its own introduce pseudouridines at position 55 in the T arm of tRNAs like its bacterial homologue TruB[17]. This activity is greatly enhanced by the addition of Nop10 and Gar1[18,19]. The significance of this guide-independent activity of Cbf5 is not clear as it has been demonstrated that tRNAs are pseudouridylated *in vivo* by another archaeal enzyme, Pus10[20].

Here, we ask the question why Cbf5 requires additional proteins, in particular Nop10 and Gar1, for its optimal function. Answering this question is not possible by investigating the guide RNA-dependent reaction of the H/ACA small ribonucleoprotein complex, as it loses its complete guide-dependent activity without Nop10. Therefore, we dissected the role of Nop10 and Gar1 for the guide-independent tRNA modification by Cbf5. Our results clearly show that Nop10 and Gar1 not only increase Cbf5's affinity to tRNA, but that they also enhance its catalytic activity.

Results

Multiple-turnover catalysis of tRNA modification by Cbf5 in absence and presence of Nop10 and Gar1. In order to understand the contribution of proteins Nop10 and Gar1 on the pseudouridylation activity of Cbf5, a highly-purified *Pyrococcus furiosus* model system was used, similarly to previous studies[13–15]. Each protein was individually expressed in *Escherichia coli*, and cells expressing the respective proteins were combined during cell opening to allow for formation of protein complexes. Subsequently, the individual proteins (Cbf5, Gar1) or protein complexes (Cbf5-Nop10, Cbf5-Nop10-Gar1) were purified by affinity and size-exclusion chromatography utilizing the hexa-histidine tag engineered onto the N-terminus of Cbf5 or Gar1. This purification strategy is essentially identical to previously published methods[13]. All proteins were more than 95% pure as judged by SDS-PAGE. To study Cbf5's activity in modifying archaeal tRNA, *P. furiosus* tRNA^{Asp}, a substrate of Cbf5[17], was generated by *in vitro* transcription using [C5-^{3}H]UTP and subsequently purified by anion exchange chromatography.

To verify the activity of the *in vitro* reconstituted complexes, time courses of pseudouridine formation were recorded at 70°C, which has previously been shown to be the optimal temperature for Cbf5[17], and under multiple turnover conditions, i.e. with lower enzyme (10 nM) than substrate (1000 nM) concentration (Fig. 1). The extent of pseudouridylation was determined using a well-established tritium release assay detecting liberation of tritium from the C5 of the uracil base upon formation of the new C-C glycosidic bond[21]. No tritium was released from the tRNA under these conditions in the absence of proteins. Notably, more than 80% pseudouridine formation was observed after 60 min for the Cbf5-Nop10-Gar1 complex as well as the Cbf5-Gar1 complex while the Cbf5-Nop10 complex yielded 60% pseudouridine formation in 60 min. Interestingly, Cbf5 alone only reached about 20% pseudouridylation after 60 minutes of incubation. This might be attributed to the general tendency of free Cbf5 to precipitate as observed during purification. In general, our findings are consistent with previous studies which showed an increasing activity of Cbf5 upon addition of Nop10 alone, Gar1 alone, or both Nop10 and Gar1; the latter Cbf5-Nop10-Gar1 complex representing the most active complex[17–19]. However all these studies were conducted under single-turnover conditions using a large excess of enzyme over substrate. Therefore, our findings
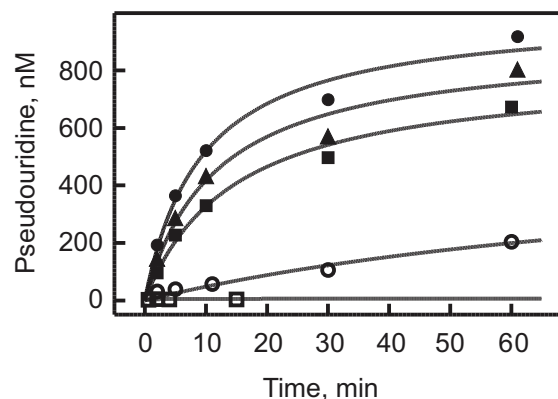

Figure 1 | Time courses of pseudouridine formation by Cbf5 alone and in the presence of Nop10 and Gar1. 1000 nM [^{3}H]tRNA was incubated at 70°C with 10 nM Cbf5-Nop10-Gar1 (closed circles), Cbf5-Gar1 (triangles), Cbf5-Nop10 (squares) or Cbf5 alone (open circles). As a control, 1000 nM [^{3}H]tRNA was incubated in reaction buffer alone (open squares). The extent of pseudouridine formation was quantified using the tritium release assay.

demonstrate for the first time that Cbf5 and its complexes with Nop10 and Gar1 are able to catalyze tRNA modification in a multiple-turnover fashion. It furthermore reveals that all of the analyzed complexes are capable of efficient product release in contrast to the guide RNA-dependent function of Cbf5 where the reaction is limited to a single round of catalysis when Gar1 is absent, presumably since the product RNA cannot dissociate from the H/ACA small ribonucleoprotein[12]. In summary, we are using a highly-active, purified reconstituted *in vitro* system capable of multiple-turnover catalysis for studying pseudouridylation by Cbf5 in presence and absence of Nop10 and Gar1.

Steady-state kinetic analysis of tRNA modification by Cbf5. In order to identify the role of Nop10 and Gar1 for tRNA modification by Cbf5, we have conducted steady-state kinetic experiments utilizing the fully active Cbf5-Nop10-Gar1 complex as well as complexes lacking either Nop10 or Gar1. We did not analyze the Cbf5 enzyme alone due to its limited activity (Fig. 1). Based on these experiments we have determined the catalytic constants (k_{cat}) as well as the Michaelis constants (K_M), which respectively provide insights into catalysis and interaction with the substrate RNA. Based on the initial, linear phase of product formation using 10 nM enzyme, the initial velocity (v_0) of the reaction could be determined by linear fitting (Fig. 2a). The respective experiments were conducted at different tRNA concentrations ranging from 150 to 3000 nM to determine the dependence of the initial velocity on the substrate concentration (Fig. 2b–d). Fitting to a Michaelis-Menten equation provided the steady-state kinetic parameters k_{cat} and K_M summarized in Table 1. Interestingly, all three analyzed complexes exhibited very similar behavior at low tRNA concentrations (< 300 nM tRNA). However, at higher tRNA concentration, the initial velocity of the Cbf5-Nop10 as well as the Cbf5-Gar1 catalyzed reaction did increase only very slightly (Fig. 2 b and c). In contrast, the Cbf5-Nop10-Gar1 complex showed a strong increase in initial velocity with higher substrate tRNA concentrations up to a velocity of 180 nM min^{-1} at 3000 nM tRNA without reaching saturation (Fig. 2d). Thus, both Nop10 and Gar1 contribute significantly to Cbf5's activity in particular at high substrate concentrations. This trend is confirmed by the quantitative analysis of the titrations, as the k_{cat} of the Cbf5-Nop10-Gar1 complex is 0.7 s^{-1}, more than threefold higher than that of Cbf5-Gar1 (0.2 s^{-1}) and about six fold larger than the k_{cat} of the Cbf5-Nop10 complex (0.11 s^{-1}). Interestingly, the effect of Nop10 and Gar1 on the Michaelis-Menten constant, K_M,
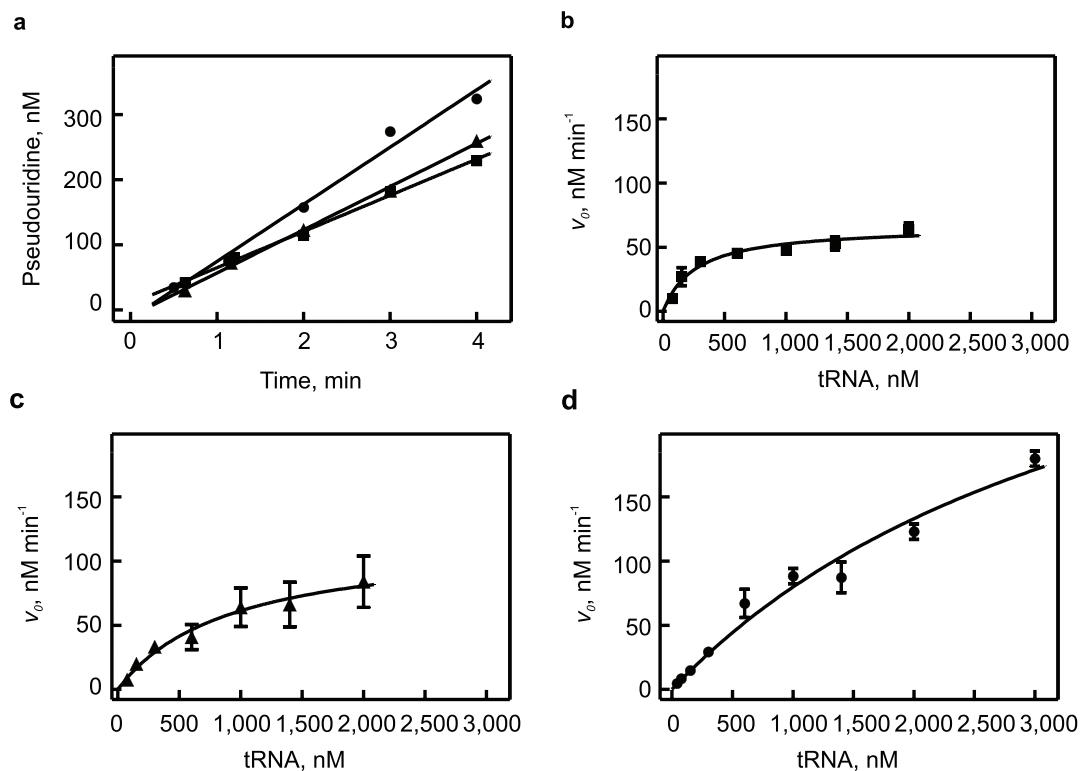
Figure 2 | Steady-state kinetic analysis of pseudouridylation by the Cbf5-Nop10-Gar1 complex and sub-complexes thereof. (a) Short time courses using 1000 nM [³H]tRNA and 10 nM enzyme to determine the initial velocity (v_0) of pseudouridine formation and its standard deviation by linear fitting. Cbf5-Nop10-Gar1 (circles), Cbf5-Gar1 (triangles), Cbf5-Nop10 (squares). Similar time courses were recorded at different tRNA concentrations, and the obtained initial velocities including standard deviations were plotted against the substrate concentration (b–d). Different complexes of Cbf5 were used as enzymes: Cbf5-Nop10 (b), Cbf5-Gar1 (c), and Cbf5-Nop10-Gar1 (d). Fitting to the Michaelis-Menten equation (smooth lines) yielded values for k_{cat} and K_M (see Table 1).

is different than on k_{cat}. The K_M for tRNA decreases from about 4000 nM for the Cbf5-Nop10-Gar1 complex to 920 nM for Cbf5-Gar1 and 260 nM for Cbf5-Nop10. This is surprising as on the first view, this would suggest that the Cbf5-Nop10-Gar1 complex is less efficient in interacting with substrate tRNA than the partially assembled complexes.

Substrate binding by Cbf5 alone and in complex with Nop10 and/or Gar1. In order to shed more light on the mechanism of substrate binding by Cbf5-Nop10-Gar1 and subcomplexes thereof, nitrocellulose filtration assays were performed to determine the dissociation constants (K_D) for tRNA^{Asp} binding. To prevent modification of the bound tRNA, we have constructed a catalytically inactive Cbf5 variant by mutating the catalytic aspartate 85 to asparagine (D85N). This renders the protein completely inactive in pseudouridylation[22] (data not shown) while retaining its RNA binding abilities (see below). Subsequent to a 10 minute incubation of 10 nM [³H]tRNA in the presence of excess protein, the reaction mixture was filtered

through a nitrocellulose membrane that retains protein and protein-bound tRNA. After washing of the membrane with reaction buffer, the amount of retained and therefore bound tRNA was determined by scintillation counting of the nitrocellulose filters. In order to assess the role of Nop10 and Gar1 for tRNA binding, we analyzed not only the Cbf5D85N-Nop10-Gar1, the Cbf5D85N-Nop10 and the Cbf5D85N-Gar1 complex, but also Cbf5D85N and Gar1 alone as Gar1 has been shown to bind RNA[23]. For all proteins and protein complexes tested, about 80% of the tRNA was bound to protein at high protein concentrations (Fig. 3). Gar1 bound tRNA comparatively weakly (K_D of 750 nM, Table 2), and Cbf5D85N alone bound tRNA with an intermediate affinity (K_D = 235 nM). However, all other complexes of Cbf5D85N with Nop10 and/or Gar1 displayed a high affinity for tRNA ranging from 45 – 80 nM (Table 2). In comparison to Cbf5D85N alone, these results clearly show that both Nop10 and Gar1 enhance Cbf5's ability to bind tRNA to similar extent. Furthermore, these experiments demonstrate that the complete Cbf5-Nop10-Gar1 complex is fully capable of tight binding to the substrate tRNA despite its high K_M (Fig. 2 and Table 1).

The large difference between the K_D and the K_M can be explained with the high catalytic activity of the Cbf5-Nop10-Gar1 complex. Only for the classical Michaelis-Menten mechanism is the K_D ($= k_{-1}/k_1$) equal to the K_M, i.e. only if the catalytic rate constant (k_2) is low compared to dissociation of substrate (k_{-1})[24]. This is not the case for most enzymes including Cbf5-Nop10-Gar1 where K_M is influenced not only by the rate constants for substrate binding (k_1, k_{-1}), but also by the rate constant of catalysis (k_2) or other subsequent steps. For the relatively simple Briggs-Haldane mechanism, K_M is defined as $(k_{-1} + k_2)/k_1$[24]. While the exact kinetic mechanism of Cbf5-Nop10-Gar1 in modifying tRNA is not known, our data are consistent with a Briggs-Haldane mechanism. As the Cbf5-Nop10-Gar1

Table 1 | Kinetic parameters for tRNA modification by different Cbf5 complexes[a]

	K_M, nM	k_{cat}, s^{-1}	k_Ψ, s^{-1}
Cbf5-Nop10-Gar1	4000 ± 1700	0.7 ± 0.2	> 0.2
Cbf5-Gar1	920 ± 240	0.20 ± 0.03	0.06 ± 0.02
Cbf5-Nop10	260 ± 70	0.11 ± 0.01	0.07 ± 0.02
Cbf5	n.d.	n.d.	0.04 ± 0.01

n.d. – not determined.
[a]Each value for K_M, k_{cat} and k_Ψ is reported together with its standard deviation obtained from data fitting as described in the Methods.
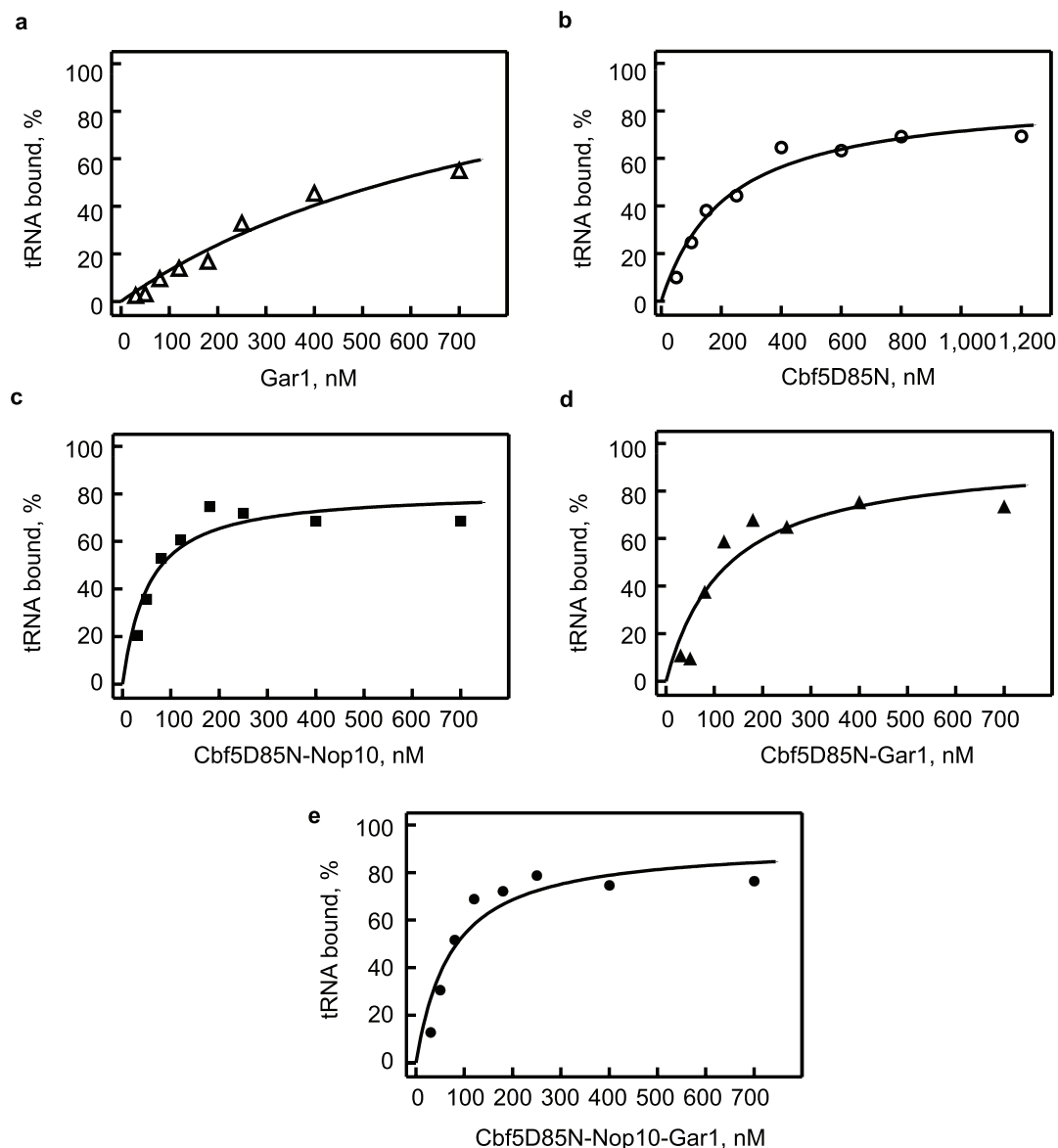
Figure 3 | Substrate tRNA binding by Cbf5 in presence and absence of Nop10 and Gar1. To determine the affinity of Cbf5 and Cbf5-complexes to unmodified substrate tRNA, [³H]tRNA was incubated with increasing concentrations of the catalytically inactive Cbf5 D85N variant and associated proteins. The percentage of bound tRNA was recorded by nitrocellulose filtration and scintillation counting. The experiment was carried out with Gar1 alone (a), Cbf5D85N alone (b), Cbf5D85N-Nop10 (c), Cbf5D85N-Gar1 (d), and Cbf5D85N-Nop10-Gar1 (e). Fitting to a quadratic function (Materials and Methods, smooth lines) provided the dissociation constant, K_D, for the interaction of Cbf5 and its complexes with substrate tRNA (see Table 2). Here, individual titrations are shown, but each experiment was repeated at least three times to determine the dissociation constants, K_D, reported in Table 2.

Table 2 | Affinity of Cbf5 complexes to substrate and product tRNA[a]

	K_D, nM (substrate tRNA)	K_D, nM (product tRNA)
Cbf5	235 ± 65	n.d.
Cbf5-Nop10-Gar1	45 ± 20	27 ± 10
Cbf5-Gar1	80 ± 25	105 ± 25
Cbf5-Nop10	50 ± 15	60 ± 20
Gar1	750 ± 300	n.d.

n.d. – not determined.
[a]Each K_D is the average of at least three different nitrocellulose filtration experiments titrating protein against tRNA. Each average K_D value is reported together with the largest standard deviation from individual filtration experiments (for details see Methods).

complex has a high catalytic constant, k_{cat}, which most likely reflects the rate constant of catalysis, k_2, it is expected that K_M increases with k_2. In contrast, the catalytic constant, k_{cat}, is rather low for the Cbf5-Nop10 complex, and hence its K_M value is in a similar order of magnitude as the K_D, i.e. the Cbf5-Nop10 complex might follow the Michaelis-Menten mechanism. In conclusion, the high K_M of the Cbf5-Nop10-Gar1 complex seems to be a result of its high k_{cat} value, or in other words the high catalytic activity of the Cbf5-Nop10-Gar1 complex is achieved by "sacrificing" the K_M value for tRNA. Notably, this property does not necessarily have to apply to the complete H/ACA small ribonucleoprotein as it employs a different mechanism for substrate RNA binding based on guide RNA.

Single-turnover tRNA modification by Cbf5 and Cbf5 complexes. Next, we asked whether Gar1 could influence the release of product tRNA as it has been implicated in product release during the

guide-dependent activity of the H/ACA small ribonucleoprotein[12]. For this purpose, pseudouridylation assays were conducted under single-turnover conditions, i.e. with an excess of enzyme (5 μM) over [3H]tRNA (0.6 μM). Under these conditions, the tritium release assay detects the appearance of the enzyme-product complex as the active site is accessible to water and the released tritium can easily escape the active site. Therefore, the measured rate constant is independent of product release in contrast to the k_{cat} measured under multiple round conditions. If product release is rate-limiting under the multiple turnover conditions, for example upon omission of Gar1, the k_{cat} would be lower than the single-round rate constant of pseudouridine formation (k_ψ). It is therefore the aim of these single-round experiments to assess whether product release is limiting by comparing k_ψ and k_{cat}. For these experiments, very short time courses have to be measured as the reaction is expected to be rather fast. Usually we would achieve this by using the rapid-mixing quench flow apparatus; however, this is not feasible at 70°C. Therefore, the experiments were performed by hand allowing at least a rough estimation of single-round pseudouridylation rate constants (k_ψ). Again, all Cbf5 complexes with Nop10 and/or Gar1 achieved 80% or more product formation in a short time (Fig. 4). Interestingly, Cbf5 alone was able to form pseudouridines with a rate of 0.04 s^{-1} under these conditions, but failed to convert more than 30% of all tRNAs which again might be explained by an instability of Cbf5 during the course of the experiment. As expected based on the k_{cat}, the complete Cbf5-Nop10-Gar1 complex had converted all substrate to product within the first 10 seconds, thus indicating that the single-round rate constant is at least 0.2 s^{-1} or larger. Interestingly, upon omitting Gar1, the Cbf5-Nop10 complex displayed a single-round rate constant of 0.07 s^{-1} which is very similar to the k_{cat} value of 0.11 s^{-1} for this complex given the precision of the measurements (Table 1). This clearly demonstrates that product release is fast for the Cbf5-Nop10 complex. Therefore, Gar1 is not involved in tRNA product release in contrast to its function in the guide-dependent reaction[12]. For the Cbf5-Gar1 complex, the single-round rate constant is 0.06 s^{-1} and therefore also in a comparable magnitude to the k_{cat} (Table 1). This indicates that Nop10 is also not involved in product release.

Interaction of Cbf5 complexes with modified product tRNA and H/ACA guide RNA. Based on previous studies reporting that pseudouridine synthases can bind modified product tRNA[25], we
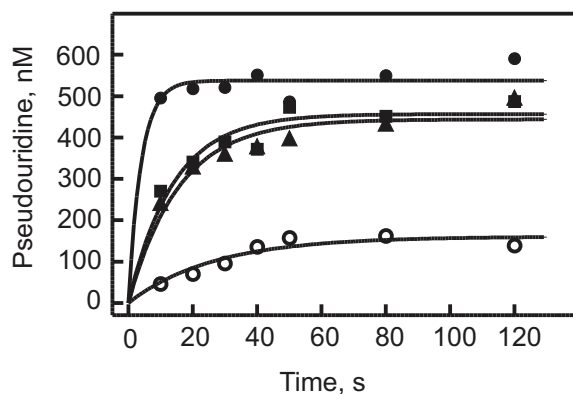

Figure 4 | Effect of Nop10 and Gar1 on a single-round of pseudouridine formation by Cbf5. 0.6 μM of [3H]tRNA was incubated with 5 μM of Cbf5 and accessory proteins at 70°C, and pseudouridine formation was determined using the tritium release assay. Under these conditions, each Cbf5 enzyme can only modify a single tRNA. The tRNA was reacted with Cbf5-Nop10-Gar1 (closed circles), Cbf5-Gar1 (closed triangles), Cbf5-Nop10 (closed squares), or Cbf5 alone (open circles). The time courses were fit to a single-exponential equation to estimate the single-turnover rate constant of pseudouridine formation, k_ψ (Table 1).

next examined whether this is also the case for Cbf5. To this end, the nitrocellulose filtration assays with [3H]tRNA were repeated in the presence of active, wild-type Cbf5 in complex with Nop10 and/or Gar1. As shown in the single-turnover pseudouridylation assay (Fig. 4), all uridines should be converted to pseudouridines by the Cbf5-Nop10, Cbf5-Gar1 and Cbf5-Nop10-Gar1 complexes during the 10 minute incubation period at 70°C allowing the measurement of modified product tRNA binding. Interestingly, all Cbf5 complexes again displayed relatively tight tRNA binding reaching maximal binding at protein concentrations of about 100 nM (Fig. 5). Fitting of the data revealed the dissociation constants (K_D) as summarized in Table 2. The comparison to the respective affinities for unmodified substrate tRNA reveals that Cbf5 complexes with Nop10 and/or Gar1 bind with similar affinities to substrate and product tRNA. Notably, tight binding of the product tRNA does not exclude rapid product release; instead it is likely that product binding is a dynamic equilibrium with rapid dissociation and re-association of the tRNA.

Lastly, we were asking how the interaction of the Cbf5-Nop10-Gar1 complex with tRNA compares to its interaction with H/ACA guide RNA as it occurs in the archaeal cell. Therefore, [3H]-labeled H/ACA guide RNA Pf4[26] was prepared and used in nitrocellulose filtration assays with Cbf5-Nop10-Gar1. The titration revealed that H/ACA guide RNA binds tightly to Cbf5-Nop10-Gar1 reaching the end level already at 100 nM of protein. The dissociation constant for the interaction of Cbf5-Nop10-Gar1 with H/ACA guide RNA Pf4 is 21 ± 8 nM as determined in three independent experiments. Hence, Cbf5-Nop10-Gar1 binds guide RNA as tight as tRNA (see Table 2).

Discussion

Here, we present the first quantitative analysis of guide-independent pseudouridine formation by archaeal Cbf5 in presence and absence of its accessory proteins Nop10 and Gar1. Our findings demonstrate that both Nop10 and Gar1 enhance Cbf5's catalytic activity. Furthermore, they improve Cbf5's interaction with its substrate tRNA. In contrast to the guide-dependent reaction, Gar1 does not affect product release by Cbf5. All Cbf5 complexes are capable of tight-binding to both the substrate and the product tRNA. These quantitative findings allow for the first time a detailed insight into the role of the accessory proteins Nop10 and Gar1.

Our results unambiguously show that lack of either Nop10 or Gar1 from the full Cbf5-Nop10-Gar1 complex reduces the catalytic constant, k_{cat}, revealing a role of Nop10 and Gar1 in enhancing the catalytic ability of Cbf5. In general, the active site of pseudouridine synthases contains three residues that have been implicated in catalysis: an asparatate that is essential for catalysis as well as a tyrosine (phenylalanine in TruD) and an arginine or lysine interacting with the catalytic aspartate[1]. Our findings raise the question of how Nop10 and Gar1 can influence the active site of Cbf5.

The different crystal structures of Cbf5-Nop10-Gar1 support the hypothesis that Nop10 and Gar1 may influence all three active site residues of Cbf5 and may contribute to positioning of the substrate tRNA. As seen in the crystal structures of Cbf5-Nop10-Gar1, Nop10 binds in the vicinity of Cbf5's active site whereas Gar1 can interact with Cbf5's thumb loop, but is not close to the active site of Cbf5 (Fig. 6)[13,27]. Based on these structural constraints, it is highly unlikely that either Nop10 or Gar1 contribute a residue directly to the active site which is also in accordance with the observation that significant catalytic activity is retained upon loss of Nop10 or Gar1. Instead, we hypothesize that Nop10 and Gar1 are indirectly influencing Cbf5's activity. For Nop10, it has already been proposed based on the crystal structures that it stabilizes the active site of Cbf5[28]. Nop10's linker region directly interacts through a so-called proline spine with the conserved motif I in Cbf5 which is located next to the active site and contacts the catalytic aspartate residue[29]. Additionally, the N-terminal domain, specifically the conserved tyrosine 14 of Nop10 (*P. furiosus* numbering as in Duan et al.[12]), contacts the conserved
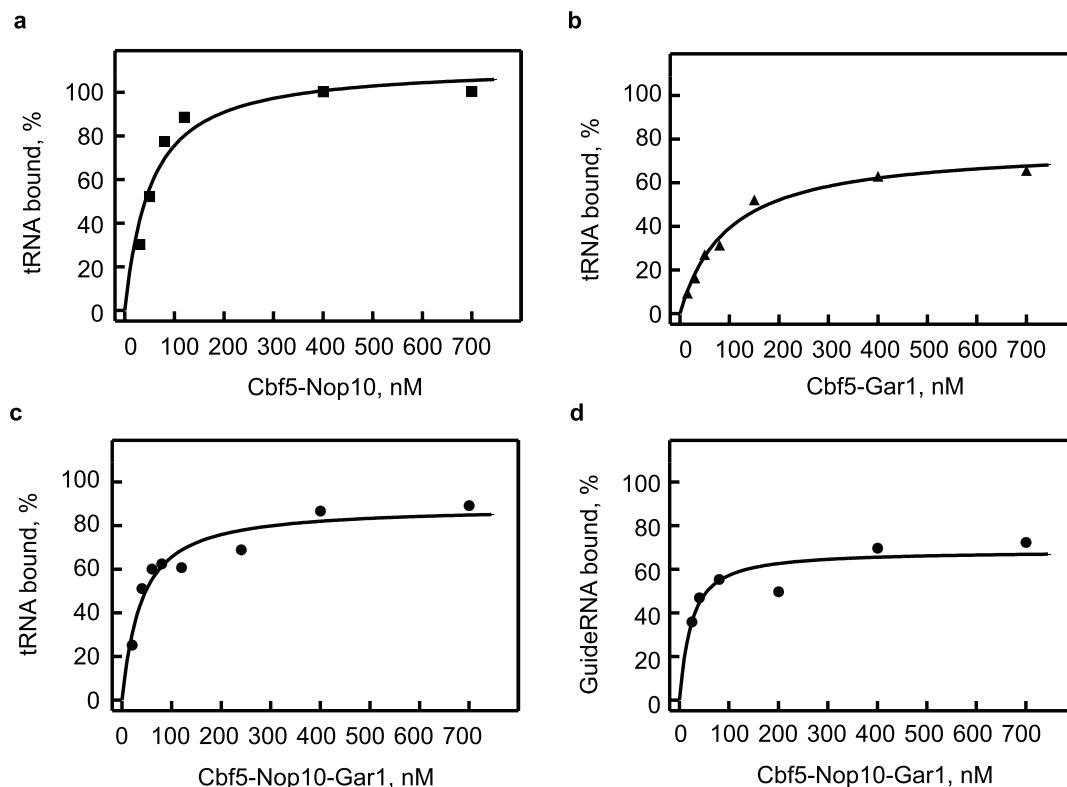
Figure 5 | Binding of modified product tRNA in comparison to H/ACA guide RNA by Cbf5 in presence and absence of Nop10 and Gar1. [3H]tRNA or [3H] H/ACA guide RNA was incubated at 70°C for 10 minutes with increasing concentrations of wild-type, active Cbf5-Nop10-Gar1 as well as complexes missing Nop10 or Gar1 followed by nitrocellulose filtration and scintillation counting to determine the percentage of bound product tRNA. The tRNA experiment was performed with Cbf5-Nop10 (a), Cbf5-Gar1 (b), and Cbf5-Nop10-Gar1 (c). The H/ACA guide RNA was bound to Cbf5-Nop10-Gar1 (d). Smooth lines are the result of fitting to a quadratic function yielding the dissociation constants, K_D, for product tRNA binding (see Table 2) and H/ACA guide RNA binding (21 ± 8 nM). Again individual, representative titrations are shown.

valine 114 in β4 of Cbf5 which is next to the conserved tyrosine 113 residue that has been implicated in catalysis[28]. Hence the effect of Nop10 on Cbf5's catalytic ability might result from a stabilization of motif I in Cbf5 and β4 thereby correctly positioning the active site residues aspartate 85 and tyrosine 113 (Fig. 6). Gar1 contacts the C-terminus of Cbf5's helix 5 which contains arginine 184 at its N-terminus that is the third of the active site residues. Additionally, Gar1 can interact with Cbf5's thumb loop in the so-called open conformation[13] and maintains interactions with Cbf5's strand β7 preceding the thumb loop in the closed conformation[12]. As the thumb loop interacts with substrate RNA in presence of guide RNA[13], it can be envisioned that Gar1's interaction with β7 could also help to correctly position tRNA in Cbf5's active site (Fig. 6). Thus, Gar1 could influence the active site geometry of Cbf5 by correctly positioning helix 5 of Cbf5 and thereby the catalytic arginine, and it could indirectly enhance catalysis by substrate positioning with the help of the thumb loop.

The finding that Nop10 and Gar1 enhance Cbf5's catalytic activity during tRNA modification likely also applies to the guide-dependent pseudouridylation by Cbf5. Both the guide-dependent and the guide-independent reaction analyzed here are taking place in the same active site of Cbf5; and Nop10 and Gar1 interact in the same way with Cbf5 in the absence and presence of guide RNA as evident upon comparing the isolated Cbf5-Nop10-Gar1 structure and the full H/ACA small ribonucleoprotein[13,27]. Therefore, we hypothesize that the roles of Nop10 and Gar1 in stabilizing Cbf5's active site during catalysis also hold true for the guide-dependent reaction. Notably, it would not have been possible to identify these functions of Nop10 and Gar1 by studying the guide-dependent reaction as lack of Nop10 completely inhibits pseudouridine formation[14,15] and lack of Gar1

limits the reaction to a single round[12]. Our findings do not exclude other roles of Nop10 and Gar1 in the guide-dependent reaction in particular for substrate RNA binding and product release which might be substantially different from Cbf5's interactions with tRNA.

Notably, Cbf5-Nop10-Gar1 displays a similar catalytic constant of about 0.7 s⁻¹ to the rate constants of pseudouridylation by bacterial pseudouridine synthases TruB, TruA and RluA (0.35 to 0.7 s⁻¹)[11]. It has been previously discussed that this relatively low catalytic rate constant will most likely apply to all bacterial stand-alone pseudouridine synthases. The findings for Cbf5-Nop10-Gar1 now suggest that uniform slow catalysis is a general feature of pseudouridine synthases that holds true also for complex pseudouridine synthases such as Cbf5. Possibly, such a slow rate of catalysis is a result of the chemical mechanism required for pseudouridine formation. Pseudouridylation consists of at least cleavage of the glycosidic bond, rotation of the uracil base and formation of the new C-C glycosidic bond, and this reaction is presumably catalyzed by the same mechanism in all pseudouridine synthases sharing a conserved catalytic domain and conserved active site residues[1]. As this is a chemically complex reaction, it might not be possible to enhance pseudouridine formation to more than 0.35 – 0.7 s⁻¹.

The nitrocellulose filtration assays reveal high-affinity equilibrium binding constants (K_D) in the low nanomolar range for both substrate and product tRNA and all Cbf5 complexes. Both Nop10 and Gar1 are able to enhance Cbf5's ability to bind tRNA as the K_Ds for the protein complexes are between 27 and 105 nM while Cbf5 alone binds tRNA with a K_D of 235 nM (Table 2). Again, this improved tRNA binding might be a result of the overall stabilization of Cbf5 by Nop10 and Gar1. Furthermore, Nop10 could directly contribute to
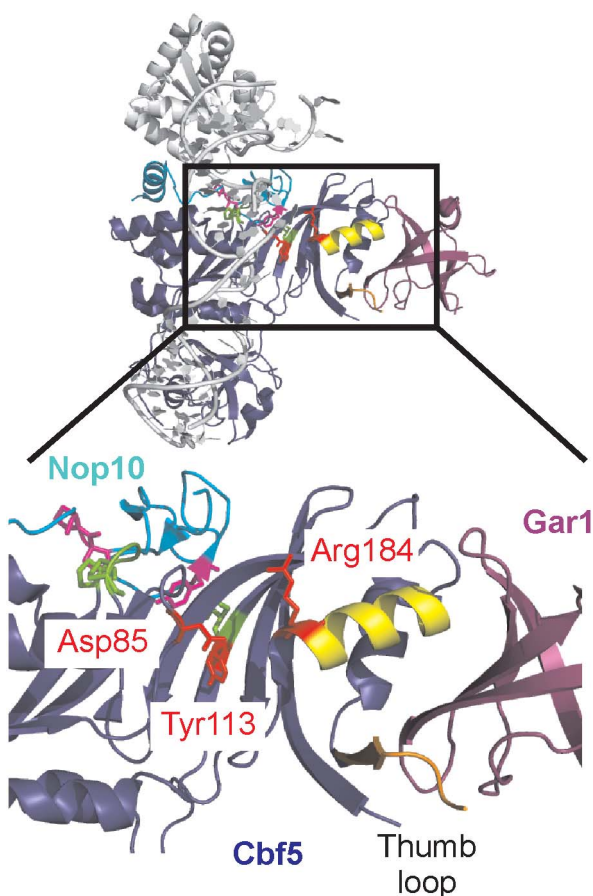
Figure 6 | Contacts between Nop10 and Gar1 and the active site of Cbf5. The upper panel shows the structure of the complete H/ACA small ribonucleoprotein with guide RNA and L7Ae depicted in grey (PDB ID: 2HVY[13]); the active site of Cbf5 as shown below is indicated by the boxed area. The active site residues of Cbf5 (Asp85, Tyr113, and Arg184) are shown in red. Nop10 is depicted in cyan and Gar1 in purple. Residues of Nop10 indicated in pink are in contact with Cbf5 residues shown in green that are in the direct neighborhood of the active site residues Asp85 and Tyr113. Gar1 contacts helix 5 of Cbf5 (yellow) that contains the active site Arg184 at its N-terminus; furthermore Gar1 interacts with Cbf5's β7 strand preceding the thumb loop (orange) which can interact with the substrate RNA. These contacts can potentially contribute to the stabilization of Cbf5's active site by Nop10 and Gar1. The figure was prepared using PyMol (www.pymol.org).

tRNA binding as it also forms contacts to the guide RNA in the H/ACA small ribonucleoprotein[13]. Gar1 does not contact the guide RNA and might not be directly involved in tRNA binding; accordingly, at least for product binding, Gar1's effect on the affinity of Cbf5 for tRNA seems to be smaller than the effect of Nop10 (Table 2). Overall, our findings suggest that, although tRNA is not the *in vivo* substrate of Cbf5, Cbf5 has retained the ability to interact with tRNA similarly as its bacterial homologue TruB. Interestingly, Cbf5 alone and its complexes display an even higher affinity for tRNA than TruB[11,25]. Based on a structural comparison of Cbf5 with TruB and its interaction with tRNA[13,30], it is likely that the tRNA binding site on Cbf5 overlaps with the guide RNA binding site. Therefore, the high tRNA affinity of Cbf5 might reflect the ability of Cbf5 to tightly bind H/ACA guide RNA (Fig. 5d). Furthermore, it is not surprising that binding of modified product tRNA to the Cbf5 complex is very similar to binding of unmodified substrate tRNA as the introduction of pseudouridine represents a relatively minor change to the overall tRNA structure. Similarly, binding of product tRNA has previously been observed for TruB[25].

In contrast to Gar1's function during the guide-dependent reaction, Gar1 is not involved in product release from Cbf5 for the guide-independent modification of tRNA[12]. Our data clearly show that multiple rounds of catalysis can occur rapidly in the absence of Gar1, i.e. for the Cbf5-Nop10 complex. Also, the single-round rate constant of catalysis, k_Ψ, is similar to the multiple round catalytic constant, k_{cat}, for the Cbf5-Nop10 complex indicating that product release is not rate-limiting. In fact, product release is also rapid for Cbf5-Nop10-Gar1 and Cbf5-Nop10, i.e. rapid tRNA release seems to be a general feature of the guide-independent reaction. This differential function of Gar1 for product release in the guide-dependent and –independent RNA modification can best be explained by a different mode of substrate binding. In the presence of a guide RNA, the substrate RNA is held in place through several base-pairs. In contrast, the tRNA directly interacts with the proteins, predominantly Cbf5 and maybe Nop10, and these contacts might be easier to break during release of the product tRNA.

In summary, the first quantitative analysis of pseudouridine formation by Cbf5-Nop10-Gar1 reported here reveals that both Nop10 and Gar1 can stabilize the active site of Cbf5 thereby enhancing its catalytic activity. We hypothesize that this is a general feature of Nop10 and Gar1 which could also indirectly contribute to catalysis during the guide-dependent reaction. Furthermore, we demonstrate for the first time that Cbf5-Nop10-Gar1 complexes have very high affinities for tRNA in the low nanomolar range, but are capable of rapidly releasing modified product tRNA. As Cbf5-Nop10-Gar1 displays an equally high affinity to H/ACA guide RNA as to tRNA, we suggest that Cbf5-Nop10-Gar1 might be mostly found bound to guide RNA in the archaeal cell and might therefore not be available for modifying tRNA which is instead catalyzed by Pus10 *in vivo*. This quantitative characterization of the complex archaeal pseudouridine synthase Cbf5 in tRNA modification paves the way for further studies into the mechanism of guide-RNA dependent pseudouridine formation by the H/ACA small ribonucleoprotein complex.

Methods

Buffers and reagents. Reaction buffer: 20 mM HEPES-KOH pH 7.0, 1.5 mM MgCl$_2$, 150 mM KCl, 0.1 mM EDTA. Nucleotide triphosphates and guanine monophosphate for *in vitro* transcription, and inorganic pyrophosphatase were from Sigma; all other enzymes were from Fermentas. Chemicals were purchased from VWR, DNA oligos were obtained from IDT and [C5-³H] UTP (MT 553) was from Moravek.

Molecular cloning and mutagenesis. The genes encoding the proteins Cbf5, Nop10, Gar1 and Pus10 were amplified from *P. furiosus* genomic DNA (ATCC, 43587D-5) using the following primers (restriction site in italics):
Cbf5 sense (BamHI) 5′-*GGATCC*GGCGAGAGACGAGGTAAGAAG-3′
Cbf5 antisense (SalI) 5′-*GTCGAC*TTAGCTTCTATCTCTTTTTTCCC-3′
Nop10 sense (BglII) 5′-CCCG*AGATCT*CAGGTTTAGGATAAGGAAGTGTC-3′
Nop10 antisense (XhoI) 5′-CATT*CTCGAG*TCATTTTTCCTTCCTCCCTA-3′
Gar1 sense (histag, NheI) 5′-ATG*GCTAGC*GAAAAACAGGGTGAAAAAATG-3′
Gar1 sense (no his, NcoI) 5′-GCG*CCATGG*CGAAAAACAGGGTGAAAAAATG-3′
Gar1 antisense (BamHI) 5′-TTC*GGATCC*TCATCTATTCAGCCTTTTCTTC-3′
Subsequently, the genes were inserted by blunt-end ligation into SmaI restricted pUC19 plasmid. Using restriction sites added through the primers, the genes were removed from the pUC19 plasmid and inserted into an expression vector which had been double-restricted with the appropriate enzymes and gel purified. This generated the following plasmids: pETDuet1-PfCbf5 (gene in multiple cloning site I including an N-terminal hexahistidine tag), pETDuet1-PfNop10(nohis) (gene in multiple cloning site II without tag), pET28a-PfGar1 (including N-terminal hexahistidine tag), and pET28a-PfGar1(nohis) (without tag used for purification in complex with Cbf5). To generate catalytically inactive variant of Cbf5, quikchange mutagenesis was applied to change the catalytic aspartate to asparagine generating plasmid pETDuet1-PfCbf5D85N. All plasmids were verified by sequencing (Macrogen).

Protein expression and purification. For protein expression, plasmids were individually transformed into Rosetta 2(DE3) competent *E. coli* cells (EMD Bioscience). To express Cbf5 and Nop10, cells were grown in LB medium supplemented with100 μg/mL ampicillin; for Gar1 expression, LB medium contained 50 μg/mL kanamycin. At an OD$_{600}$ of ~0.6, protein expression was induced by the addition of isopropyl β-D-1-thiogalactopyranoside (IPTG) to a final concentration of 1 mM. In case of Gar1, cells were transferred to 30°C prior to the induction. Cells were

harvested three hours after induction by centrifugation at 5,000 ×g for 15 min, flash frozen and stored at −80°C.

Cbf5 and Gar1 were individually purified. For purification of Cbf5-Nop10 and Cbf5-Nop10-Gar1 complexes, cells were mixed to allow formation of the protein complex during cell opening similar as in previous reports[13]. In all cases, cells were resuspended in 5 mL/g Buffer A1 for purification of Cbf5-Nop10 and Cbf5-Nop10-Gar1 (25 mM sodium phosphate buffer (pH 7.6), 1 M NaCl, 5% (v/v) glycerol, 30 mM imidazole and 0.1 mM phenylmethylsulfonyl fluoride (PMSF)) or Buffer A2 for purification of Cbf5 and Gar1 alone (20 mM Tris-HCl pH 8.0, 300 mM KCl, 5 mM β-mercaptoethanol, 5% (v/v) glycerol, 30 mM imidazole, 0.1 mM PMSF). Cells were lysed for 30 min on ice by adding 1 mg/mL lysozyme followed by addition of sodium deoxycholate (12.5 mg/g cells) and further incubation for 15 min on ice. The solution was sonicated five times for 1 min each (intensity level 6, duty cycle 60%, Branson Sonifier) and centrifuged for 45 min at 30,000 ×g, 4°C. The lysate was then subjected to heat denaturation at 75°C for 15 min followed by centrifugation for 30 min at 30,000 ×g, 4°C. For purification of Cbf5 alone, the heat denaturation step was omitted since we observed that this step rendered the protein inactive. The cleared lysate was loaded onto a 5 mL Ni²⁺ Sepharose column (GE Healthcare) using a BioLogic LP chromatography system (BioRad) and washed extensively with Buffer A. The protein was subsequently eluted with a linear gradient (50 mL) to Buffer B (same as A except for 500 mM imidazole and no PMSF). For purification of Cbf5, glycerol was immediately added to fractions to a final concentration of 20% (v/v). Peak fractions were analyzed by 15% SDS-PAGE for Cbf5 and Gar1 purifications or 16.5% Tris-Tricine PAGE for complexes containing Nop10, pooled and concentrated by ultrafiltration (Vivaspin MWCO 30,000 or 10,000). Next, the protein was re-buffered either by ultrafiltration or by size exclusion chromatography using a Superdex 75 column (XK26/100 column, GE Healthcare) in Buffer C (20 mM HEPES-KOH pH 7.5, 600 mM KCl, 1 mM EDTA, 20% (v/v) glycerol) at a flow rate of 1 mL/min (BioLogic DuoFlow chromatography system). Peak fractions were concentrated as before, flash frozen and stored in aliquots at −80°C.

Protein concentration was determined photometrically at 280 nm using a molar extinction coefficient of 46,410 M^{-1} cm^{-1} for Cbf5, 9,970 M^{-1} cm^{-1} for Nop10, and 11,460 M^{-1} cm^{-1} for Gar1 (calculated using ProtParam[31]), while concentration of Gar1 alone was also determined at 210 nm using the extinction coefficient of 20.5 mg^{-1} ml cm^{-1}. The catalytically inactive mutant (D85N) of Cbf5 was purified either alone or in combination with Gar1 and/or Nop10, essentially in the same way as explained above.

In vitro transcription and purification of tRNA and H/ACA guide RNA. A plasmid, called pIDT-Smart-PftRNA^{Asp}, encoding a T7 promoter followed by the gene for *P. furiosus* tRNA^{Asp} was purchased from Integrated DNA Technology. To generate H/ACA guide RNA, the sequence for *P. furiosus* H/ACA guide RNA Pf4 (5′-AAUGCCCCUCCCCUCUCACACCCCCGUGAGAAGUGAGCGGGGGG-CGGUCGGGGAGGGGACAUCA-3′)[26] as well as a T7 promoter was assembled using overlapping oligos and cloned into a pUC19 vector. The template for the *in vitro* transcription of tRNA^{Asp} and Pf4 guide RNA was generated by PCR amplification from the corresponding plasmids using methylated reverse primers to precisely terminate transcription[32]. The *in vitro* transcription was performed using the PCR template (10% (v/v)) in transcription buffer (40 mM Tris-HCl pH 7.5, 15 mM MgCl₂, 2 mM spermidine, 10 mM NaCl, 10 mM DTT) with 3 mM ATP, CTP and GTP each, and 0.1 mM [C5-³H]UTP (23.9 Ci/mmole), 5 mM GMP, 0.01 U/μL inorganic pyrophosphatase, 0.3 μM T7 RNA Polymerase and 0.12 U/μL RNase inhibitor at 30°C for 4 h. The H/ACA guide RNA was *in vitro* transcribed under similar conditions at 20°C over night. Following the *in vitro* transcription, the template was digested with 2 U/mL DNaseI (Fermentas) for 1 h at 37°C, and the RNA was purified with a Nucleobond AX100 column (Macherey-Nagel) using equilibration buffer R0 (100 mM Tris-acetate pH 6.3, 10 mM MgCl₂, 15% (v/v) ethanol), washing buffer R1 (R0 with 300 mM KCl) and elution buffer R3 (R0 with 1150 mM KCl). The RNA was concentrated by isopropanol precipitation and dissolved in H₂O. The tRNA concentration was determined photometrically at 260 nm using the extinction coefficient 5×10⁵ M^{-1} cm^{-1}. The specific activity of the purified [³H]tRNA^{Asp} and [³H] guide RNA was determined by scintillation counting.

Nitrocellulose filtration. Prior to all experiments, [³H]tRNA^{Asp} and proteins were pre-incubated at 70°C for 5 min. To allow the tRNA to bind to protein, 5 or 10 nM [³H]tRNA^{Asp} was incubated with 0 – 700 nM protein or protein complex in reaction buffer for 10 min at 70°C. The complete 50 μL reaction mixture was then filtered through a nitrocellulose membrane followed by washing of the membrane with 1 mL cold reaction buffer. Membranes were dissolved for 30 min in 10 mL EcoLite scintillation cocktail (EcoLite (+), MP Biomedical), and the amount of tRNA bound to the protein retained on the membrane was determined by scintillation counting (Perkin-Elmer Tri-Carb 2800TR liquid scintillation analyzer). In order to obtain the dissociation constant (K_D), the increase in the fraction of bound tRNA as a function of the protein concentration was analyzed by fitting to a quadratic equation with [RNA] = 5 or 10 nM:

$$P_{bound} = Amp \times \left[(K_D + [RNA] + [protein])/2 - \left\{ (K_D + [RNA] + [protein])^2/4 - [protein] \times [RNA]^{0.5} \right\} \right]$$

Where P_{bound} is the percentage of bound tRNA, and Amp is the amplitude or final level of bound tRNA. Each titration was repeated at least three times; the K_D and its standard deviation was determined for each titration by fitting in GraphPad Prism. The average K_D including the largest standard deviation of individual titrations

(which is larger than the standard deviation between the K_Ds of individual titrations) is reported in Table 2.

Tritium release assay. For Michaelis-Menten titrations, different concentrations of [³H]tRNA^{Asp} (100 – 3000 nM) were incubated with 10 nM enzyme in reaction buffer plus 0.2% (w/v) bovine serum albumin at 70°C. For single-turnover experiments, 600 nM [³H]tRNA^{Asp} were incubated with 5 μM enzyme at 70°C. Samples were removed at the desired time points and added to 5% (w/v) activated charcoal (Norit A, EMD, CX0655-1) in 0.1 M HCl. Following centrifugation at 10,000 ×g for 2 min, the supernatant was added to 0.5 mL fresh 5% (w/v) activated charcoal in 0.1 M HCl, mixed and centrifuged again. The supernatant was filtered through a glass wool plugged in a 1 mL micropipet tip, and 0.8 mL of the resulting filtrate was then used for scintillation counting in 4 mL EcoLite scintillation cocktail. Each time course was repeated at least three times to determine the initial velocity, v_0, by linear fitting. The dependence of the initial rates v_0 on the tRNA concentration was analyzed by fitting the data in GraphPad Prism using the Michaelis-Menten equation $v_0 = V_{max}[S]/(K_M + [S])$, and the catalytic constant, k_{cat}, was determined by dividing v_{max} by the enzyme concentration (10 nM). The single-turnover experiments were analyzed by fitting the data to a single-exponential equation

$$Pseudouridine = Amp - Amp \times \exp(-k_\psi \times t)$$

where Amp represents the amplitude and k_ψ is the single-turnover rate constant of pseudouridine formation. In Table 1, the values for K_M, k_{cat} and k_ψ are stated along with the standard deviation for each parameter obtained by fitting in GraphPad Prism.

1. Hamma, T. & Ferre-D'Amare, A. R. Pseudouridine synthases. *Chem Biol* **13**, 1125–1135 (2006).
2. Watanabe, Y. & Gray, M. W. Evolutionary appearance of genes encoding proteins associated with box H/ACA snoRNAs: cbf5p in *Euglena gracilis*, an early diverging eukaryote, and candidate Gar1p and Nop10p homologs in archaebacteria. *Nucleic Acids Res* **28**, 2342–2352 (2000).
3. Ganot, P., Bortolin, M. L. & Kiss, T. Site-specific pseudouridine formation in preribosomal RNA is guided by small nucleolar RNAs. *Cell* **89**, 799–809 (1997).
4. Ni, J., Tien, A. L. & Fournier, M. J. Small nucleolar RNAs direct site-specific synthesis of pseudouridine in ribosomal RNA. *Cell* **89**, 565–573 (1997).
5. Lafontaine, D. L., Bousquet-Antonelli, C., Henry, Y., Caizergues-Ferrer, M. & Tollervey, D. The box H + ACA snoRNAs carry Cbf5p, the putative rRNA pseudouridine synthase. *Genes & Development* **12**, 527–537 (1998).
6. Charette, M. & Gray, M. W. Pseudouridine in RNA: what, where, how, and why. *IUBMB Life* **49**, 341–351 (2000).
7. Yang, C., McPheeters, D. S. & Yu, Y. T. Psi35 in the branch site recognition region of U2 small nuclear RNA is important for pre-mRNA splicing in *Saccharomyces cerevisiae*. *J Biol Chem* **280**, 6655–6662 (2005).
8. Liang, X. H., Liu, Q. & Fournier, M. J. rRNA modifications in an intersubunit bridge of the ribosome strongly affect both ribosome biogenesis and activity. *Molecular Cell* **28**, 965–977 (2007).
9. McDonald, M. K., Miracco, E. J., Chen, J., Xie, Y. & Mueller, E. G. The Handling of the Mechanistic Probe 5-Fluorouridine by the Pseudouridine Synthase TruA and Its Consistency with the Handling of the Same Probe by the Pseudouridine Synthases TruB and RluA. *Biochemistry* (2010).
10. Miracco, E. J. & Mueller, E. G. The products of 5-fluorouridine by the action of the pseudouridine synthase TruB disfavor one mechanism and suggest another. *Journal of the American Chemical Society* **133**, 11826–11829 (2011).
11. Wright, J. R., Keffer-Wilkes, L. C., Dobing, S. R. & Kothe, U. Pre-steady-state kinetic analysis of the three *Escherichia coli* pseudouridine synthases TruB, TruA, and RluA reveals uniformly slow catalysis. *RNA* **17**, 2074–2084 (2011).
12. Duan, J., Li, L., Lu, J., Wang, W. & Ye, K. Structural mechanism of substrate RNA recruitment in H/ACA RNA-guided pseudouridine synthase. *Molecular Cell* **34**, 427–439 (2009).
13. Li, L. & Ye, K. Crystal structure of an H/ACA box ribonucleoprotein particle. *Nature* **443**, 302–307 (2006).
14. Baker, D. L. *et al.* RNA-guided RNA modification: functional organization of the archaeal H/ACA RNP. *Genes & Development* **19**, 1238–1248 (2005).
15. Charpentier, B., Muller, S. & Branlant, C. Reconstitution of archaeal H/ACA small ribonucleoprotein complexes active in pseudouridylation. *Nucleic Acids Res* **33**, 3133–3144 (2005).
16. Liang, B., Xue, S., Terns, R. M., Terns, M. P. & Li, H. Substrate RNA positioning in the archaeal H/ACA ribonucleoprotein complex. *Nat Struct Mol Biol* **14**, 1189–1195 (2007).
17. Roovers, M. *et al.* Formation of the conserved pseudouridine at position 55 in archaeal tRNA. *Nucleic Acids Res* **34**, 4293–4301 (2006).
18. Gurha, P., Joardar, A., Chaurasia, P. & Gupta, R. Differential roles of archaeal box H/ACA proteins in guide RNA-dependent and independent pseudouridine formation. *RNA Biol* **4**, 101–109 (2007).
19. Muller, S., Fourmann, J. B., Loegler, C., Charpentier, B. & Branlant, C. Identification of determinants in the protein partners aCBF5 and aNOP10 necessary for the tRNA:Psi55-synthase and RNA-guided RNA:Psi-synthase activities. *Nucleic Acids Res* **35**, 5610–5624 (2007).
20. Blaby, I. K. *et al.* Pseudouridine formation in archaeal RNAs: The case of *Haloferax volcanii*. *RNA* **17**, 1367–1380 (2011).

21. Cortese, R., Kammen, H. O., Spengler, S. J. & Ames, B. N. Biosynthesis of pseudouridine in transfer ribonucleic acid. *The Journal of Biological Chemistry* **249**, 1103–1108 (1974).

22. Zebarjadian, Y., King, T., Fournier, M. J., Clarke, L. & Carbon, J. Point mutations in yeast *CBF5* can abolish *in vivo* pseudouridylation of rRNA. *Mol Cell Biol* **19**, 7461–7472 (1999).

23. Bagni, C. & Lapeyre, B. Gar1p binds to the small nucleolar RNAs snR10 and snR30 *in vitro* through a nontypical RNA binding element. *J Biol Chem* **273**, 10868–10873 (1998).

24. Fersht, A. *Structure And Mechanism In Protein Science: A Guide To Enzyme Catalysis And Protein Folding.* 3rd revised edition edn, (W.H. Freeman and Company, 1998).

25. Ramamurthy, V., Swann, S. L., Paulson, J. L., Spedaliere, C. J. & Mueller, E. G. Critical aspartic acid residues in pseudouridine synthases. *J Biol Chem* **274**, 22225–22230 (1999).

26. Klein, R. J., Misulovin, Z. & Eddy, S. R. Noncoding RNA genes identified in AT-rich hyperthermophiles. *Proceedings of the National Academy of Sciences of the United States of America* **99**, 7542–7547 (2002).

27. Rashid, R. *et al.* Crystal structure of a Cbf5-Nop10-Gar1 complex and implications in RNA-guided pseudouridylation and dyskeratosis congenita. *Molecular Cell* **21**, 249–260 (2006).

28. Hamma, T., Reichow, S. L., Varani, G. & Ferre-D'Amare, A. R. The Cbf5-Nop10 complex is a molecular bracket that organizes box H/ACA RNPs. *Nat Struct Mol Biol* **12**, 1101–1107 (2005).

29. Hamma, T. & Ferre-D'Amare, A. R. The box H/ACA ribonucleoprotein complex: interplay of RNA and protein structures in post-transcriptional RNA modification. *J Biol Chem* **285**, 805–809 (2010).

30. Hoang, C. & Ferre-D'Amare, A. R. Cocrystal structure of a tRNA Psi55 pseudouridine synthase: nucleotide flipping by an RNA-modifying enzyme. *Cell* **107**, 929–939 (2001).

31. Gill, S. C. & von Hippel, P. H. Calculation of protein extinction coefficients from amino acid sequence data. *Anal Biochem* **182**, 319–326 (1989).

32. Sherlin, L. D. *et al.* Chemical and enzymatic synthesis of tRNAs for high-throughput crystallization. *RNA* **7**, 1671–1678 (2001).

Acknowledgements

Author contributions

UK designed the research, RK carried out all experiments, and UK wrote the manuscript. All authors reviewed the manuscript.

Additional information

How to cite this article: Kamalampeta, R. & Kothe, U. Archaeal proteins Nop10 and Gar1 increase the catalytic activity of Cbf5 in pseudouridylating tRNA. *Sci. Rep.* **2**, 663; DOI:10.1038/srep00663 (2012).